

## Supporting Information

### ***In Situ* Articular Cartilage Regeneration through Endogenous Reparative Cell Homing using a Functional Bone Marrow-specific Scaffolding System**

Xun Sun,<sup>†,‡,∞</sup> Heyong Yin,<sup>§,∞</sup> Yu Wang,<sup>†,∞</sup> Jiaju Lu,<sup>¶</sup> Xuezheng Shen,<sup>†</sup> Changfeng Lu,<sup>†</sup> He Tang,<sup>†</sup> Haoye Meng,<sup>†</sup> Shuhui Yang,<sup>¶</sup> Wen Yu,<sup>†</sup> Yun Zhu,<sup>#</sup> Quanyi Guo,<sup>†</sup> Aiyuan Wang,<sup>†</sup> Wenjing Xu,<sup>†</sup> Shuyun Liu,<sup>†</sup> Shibi Lu,<sup>†</sup> Xiumei Wang,<sup>\*,¶</sup> and Jiang Peng<sup>\*,†</sup>

<sup>†</sup> Institute of Orthopedics, Chinese PLA General Hospital; Beijing Key Lab of Regenerative Medicine in Orthopedics; Key Lab of Musculoskeletal Trauma & War Injuries, PLA, No.28 Fuxing Road, Beijing 100853, PR China

<sup>‡</sup> Department of Orthopedics, Tianjin Hospital, No.406 Jiefang Nan Road, Tianjin 300211, PR China

<sup>§</sup> Department of Surgery, Ludwig-Maximilians-University (LMU), Nussbaumstr. 20, Munich 80336, Germany

<sup>¶</sup> State Key Laboratory of New Ceramics and Fine Processing, School of Materials Science and Engineering, Tsinghua University, Beijing 100084, PR China

<sup>#</sup> School of Biomedical Sciences, Li Ka Shing Faculty of Medicine, University of Hong Kong, No.21 Sassoon Road, Pokfulam 999077, Hong Kong, PR China

#### **Corresponding Authors**

\*E-mail: pengjiang301@126.com (J.P.).

\*E-mail: wxm@mail.tsinghua.edu.cn (X.W.).

#### **Author Contributions**

<sup>∞</sup>Xun Sun, Heyong Yin, and Yu Wang contributed equally to this paper.

## **1. Experimental Materials and Procedures**

### **1.1. Animals.**

The experimental procedures involving laboratory animals were approved by the Institutional Animal Care and Use Committee of the Chinese PLA General Hospital and were performed in accordance with the Guidelines for the Care and Use of Laboratory Animals from the Chinese Ministry of Public Health and US National Institutes of Health. New Zealand white rabbits used in the experiments were obtained from the Laboratory Animal Research Center of Chinese PLA General Hospital and housed in a temperature-controlled environment under a 14 h/10 h light/dark cycle. All procedures described below were carried out during the light period of the cycle and all surgical procedures were performed under general anesthesia with 3% sodium pentobarbital (40 mg/kg body weight, intravenously).

### **1.2. Preparation of Peptide Solution.**

The functional motif SKP (SKPPGTSS) mimicking the bioactivity of bone marrow homing peptide (BMHP) was used to functionalize the self-assembling peptide RADA16-I by direct extension from its C-terminus to form the designer functionalized RAD-SKP peptide, which was custom-synthesized by China Peptides (Shanghai, China). The peptide solutions were prepared as described by Liu et al.<sup>1</sup> Briefly, 10 mg of peptide powder was dissolved in 1 ml of double-distilled water, sonicated for 30 min (VCX 130 PB; Sonics, Newtown, CT, USA) to obtain a 1% (w/v, pH 3–4) homogeneous peptide solutions. After filter sterilization, the peptide solutions were stored at 4°C until further use. The functionalized RAD-SKP peptide was then mixed with 1% RADA16-I solution with a volume ratio of 1:1 to obtain the functionalized RAD/SKP mixture peptide solution.

### **1.3. Fabrication of the Oriented DCM Scaffold.**

The oriented DCM scaffold was fabricated using a unidirectional solidification freeze-drying method as previously described.<sup>2-3</sup> Briefly, a decellularized porcine articular cartilage matrix microfilament suspension was prepared through physical shattering and chemical decellularization. The suspension was then added to a cylindrical mold and placed vertically on a metal plate at  $-20^{\circ}\text{C}$  for 30 min, and for another 1 h at  $-80^{\circ}\text{C}$ . Following lyophilization for 48 h under vacuum, the oriented DCM scaffold was cross-linked with exposure to ultraviolet light at 258 nm for 6 h. The scaffold with a 3-mm diameter and 1.5-mm height was sterilized by  $^{60}\text{Co}$  irradiation at 5 mRad.

### **1.4. Preparation of the Biofunctional 3D Scaffolding System.**

The DCM scaffold was further combined with pure 1% RADA16-I or the RAD/SKP mixture to prepare a control composite scaffold DCM-RAD or biofunctional marrow-specific homing scaffolding system DCM-RAD/SKP. The peptide solutions were added to perfuse the porous DCM scaffold in a cell culture dish. Next, culture medium was added to trigger peptide gelation by self-assembly inside the DCM scaffold and incubated at  $37^{\circ}\text{C}$  for 1 h to obtain a biofunctional 3D scaffolding system with gel-solid biphasic phases. The medium was changed twice more to equilibrate the gel to physiological pH and was incubated at  $37^{\circ}\text{C}$  overnight prior to *in vivo* implantation and *in vitro* experiment.

### **1.5. Characterization of the Biofunctional 3D Scaffolding System.**

AFM examination was used to observe the microstructures of the peptide nanofiber hydrogel as previously described.<sup>1</sup> Briefly, one microlitre of diluted peptide samples (1% RADA16-I, RAD-SKP, and the functionalized peptide mixtures RAD/SKP,  $20 \times$  dilutions) was dropped onto a freshly cleaved mica surface for 5 s and then rinsed with 100  $\mu\text{l}$  of distilled water to spread the peptide drop. The peptide samples were then air-dried, and images were immediately taken through a AFM

(Bruker Dimension ICON, Billerica, MA, USA) with a scanning area of  $2 \times 2 \mu\text{m}$  at scan frequency of 1.02 Hz.

Circular dichroism (CD) measurement was performed to estimate the  $\beta$ -sheet contents of the pure RADA16-I, the functionalized RAD-SKP peptide, and their mixture RAD/SKP solutions as described previously.<sup>4</sup> Briefly, peptide samples were prepared by diluting 1% peptides in Milli-Q water to a working concentration of 0.01%. Samples were analyzed at room temperature in a quartz cuvette with a path length of 1 mm and in a wavelength range 180–260 nm. The CD spectra were collected using an applied photophysics chirscan instrument (Leatherhead, UK).

SEM and stereomicroscope were used to observe the morphology and microstructures of the biofunctional 3D scaffolding system. For SEM examination, specimens were fixed in 2.5% glutaraldehyde for 2 h, dehydrated in a graded ethanol series. Once dehydrated, samples were subjected to critical point drying using a CO<sub>2</sub> critical point dryer (Samdri-PVT-3D; Tousimis, Rockville, MD, USA), coated with platinum alloy and examined using a MERLIN VP compact microscope (Carl Zeiss, Jena, Germany). For stereoscopic observation, specimens were fixed in 4% paraformaldehyde for 30 min at room temperature, and then subjected to a AXIO Zoom. V16 stereoscope with a AxioCam MRm camera for imaging process.

#### **1.6. *In vitro* Mesenchymal Stem Cells (MSCs) Recruitment.**

Rabbit MSCs were isolated from bone marrow aspirates of rabbits (2.5–3.0 kg) as previously described with ethical approval from the Institutional Animal Care and Use Committee of Chinese PLA General Hospital.<sup>9</sup> Briefly, The cells were cultured in  $\alpha$ -MEM supplemented with 10% fetal bovine serum (FBS).



*In vitro* MSC recruitment was performed to assess stem cell affinity and migration toward the scaffolds. The biofunctional DCM-RAD/SKP, DCM-RAD or DCM scaffolds (n=6) were incubated with 1 ml MSC suspension ( $1 \times 10^6$ /ml) in a tissue-culture dish (not for cell attachment). After seven days incubation, the scaffolds were washed three times with phosphate-buffered saline (PBS) and then stained using a LIVE/DEAD™ Viability/Cytotoxicity Kit (Cat# L3224; invitrogen) to visualize living and dead cells within the scaffolds. Images were taken using a Leica TCS SP8 Confocal Platform.

To demonstrate cartilage specific matrix deposition within the scaffold, immunofluorescence staining anti-collagen type II was conducted. The samples were incubated overnight at 4°C with primary antibodies against collagen type II (1:100, Cat# NBP2-33343; Novus), followed by incubation with secondary Alexa Fluor 488--conjugated antibody (Abcam, Cambridge, UK) for 60 min. Next, the samples were counter-stained with 4',6-diamidino-2-phenylindole (DAPI, Life Technologies, Carlsbad, CA, USA) and subjected to confocal imaging under a Leica TCS SP8 Confocal Platform.

### **1.7. *In Vivo* Endogenous Stem Cell Homing.**

Endogenous stem cell homing using the biofunctional scaffolding system was assessed in a rabbit osteochondral defect model. New Zealand white rabbits weighing 2.5–3.0 kg (six rabbits, n = 12 knees for each group) were used for *in vivo* experiments, and ethical approval was obtained from the Institutional Animal Care and Use Committee of Chinese PLA General Hospital. Following anesthetization with 3% sodium pentobarbital (40 mg/kg body weight, intravenously), an osteochondral defect (3 mm in diameter and 1.5 mm in depth) was created using a sterile biopsy punch in the center of the trochlear groove of both knee joints. Microfracture was performed routinely to mobilize the bone marrow. Four groups were determined according to the implants: the DCM-RAD/SKP group, in which the osteochondral defect was filled with the biofunctional DCM-RAD/SKP scaffolding system; the

DCM-RAD group, in which the defect was filled with the DCM and RADA16-I combined scaffold; and the DCM group, in which the defect was filled with the DCM scaffold alone. Microfracture alone was performed as the control (MF group). Seven days after implantation, the rabbits were sacrificed, and the knees were harvested for evaluation.

### **1.8. Lineage Tracing of Recruited Cells in the Cartilage Defect Site.**

To reveal the cell lineage recruited to the injury site, immunofluorescence staining and polymerase chain reaction (PCR) were performed. Seven days after implantation, a cylindrical tissue sample (3 mm in diameter and 1.5 mm in depth) from the defect site was harvested for further evaluation. For immunofluorescence, samples (n = 6 knees derived from six rabbits respectively for each group) were fixed in 4% paraformaldehyde for 30 min at room temperature. The target antigens were retrieved by microwaving the samples in sodium citrate buffer (10 mM sodium citrate, pH 6.0). The samples were heated in a microwave to 95–100°C for 15 min and cooled for 30 min at room temperature. Thereafter, the samples were incubated overnight at 4°C with primary antibodies (both from NOVUS Biologicals, Littleton, CO, USA) against CD90 (1:200, Cat# NB200-530) and CD29 (1:100, Cat# NB100-92076), followed by incubation with secondary Alexa Fluor 488- and 594-conjugated antibodies (all from Abcam, Cambridge, UK) for 60 min. Next, the samples were counter-stained with DAPI (Life Technologies, Carlsbad, CA, USA) and subjected to confocal imaging under a Leica TCS SP8 Confocal Platform. Total cell nuclei (DAPI) and (CD29, CD90)-double labeled cells (counter stained by DAPI) in 3 maximum intensity projection images (Figure S3) per knee with six knees per group were counted using Image Pro Plus 6.0 (IPP 6.0; Media Cybernetics).

To further confirm the existence of endogenous stem cells within the functionalized scaffolding system, PCR validation of MSC markers CD29, CD90, CD44, and CD105 was performed for the

recruited cells. Seven days after implantation, the other 6 independent cylindrical tissue samples (3 mm in diameter and 1.5 mm in depth) from the defect sites were snap-frozen in liquid nitrogen and pulverized using a mortar. Total RNA was extracted using a RNeasy Mini Kit (Qiagen), and quantified using a Nucleic Acid and Protein Analyzer (Microfuge18; Beckman-Coulter). For cDNA synthesis, 1 µg of total RNA and a ReverTra Ace® qPCR RT Kit (FSQ-101; TOYOBO) was used. Semi quantitative PCR was performed with Taq DNA Polymerase (Invitrogen) in StepOne™ Real-Time PCR System (Applied Biosystems). The primers sequences and PCR conditions are listed in Table S1.

Chondrogenic lineage gene expression was analyzed using quantitative RT-PCR. Total RNA extraction and cDNA synthesis were performed as described above. qPCR was performed using StepOne™ Real-Time PCR System (Applied Biosystems). The primers designed for qPCR are listed in Table S2. The relative gene expression was normalized to glyceraldehyde 3-phosphate dehydrogenase (GAPDH) expression and presented as the fold-change to normal articular cartilage (Sham group) using the  $\Delta\Delta C_t$  method.

### **1.9. *In Vivo* Cartilage Repair in a Rabbit Model.**

New Zealand white rabbits weighing 2.5–3.0 kg (6 rabbits, n = 12 knees per group for each time point) were used according to protocols approved by the Institutional Animal Care and Use Committee at Chinese PLA General Hospital. Animals were anesthetized with 3% sodium pentobarbital (40 mg/kg body weight, intravenously). Bilateral defects of each rabbit were performed. Rabbit knee was shaved and disinfected with 70% ethanol. After a lateral parapatellar skin incision, knee joint was exposed, and patella was dislocated laterally. An osteochondral defect (3 mm diameter and 1.5 mm depth) was created with a sterile biopsy punch in the center of the trochlear groove of both knee joints. Microfracture was performed routinely to mobilize the bone marrow. DCM, DCM-RAD, or DCM-RAD/SKP (all 3 mm in

diameter and 1.5 mm in depth) was filled into the defect. All implants were placed at the same level with the surface of the surrounding cartilage. Microfracture alone was performed as a control. After treatments, the knee joint capsule and the skin were sutured in layers. After operation, all rabbits were allowed to move freely and penicillin (80000 U) was administrated up to 3 days. Animal health conditions such as weight loss, infection were followed up closely. No rabbit underwent severe adverse events and was excluded in this study. Three and six months after implantation, the knees were harvested for further evaluation.

#### **1.10. MRI of Repaired Knees.**

At 3 and 6 months post-operation, all rabbit knees in each group (n = 12 knees for each time point) underwent MRI examination according to the protocol described by Mamisch TC et al. and Huang et al..<sup>5-6</sup> A small animal-designed 7T MRI scanner (Bruker, PharmaScan; Bruker BioSpin, Germany) with a 38-mm knee coil was used. T2 and T2 mapping sequences were conducted using the Bruker ParaVision 5.0 system. The T2 value was measured from a sagittal slice through the center of the cartilage repair site. A region of interest (ROI) was selected manually on each fitted map to encompass the full thickness depth and width of the cartilage repair. Mean T2 value (relaxation time) was recorded for each ROI.

#### **1.11. Macroscopic Evaluation of Repaired Knees.**

At 3 and 6 months post-operation, all knee samples in each group (n = 12 knees for each time point) were observed by three independent evaluators. Macroscopic scoring was performed blindly by the three evaluators and was based on the ICRS scoring system (Table S3) regarding defect filling, surface smoothness, and tissue integration.<sup>7</sup>

#### **1.12. Biomechanical Assessment of Repaired Tissue.**

At 6 months post-operation, the nanoindentation test was conducted to evaluate the biomechanical

properties of repaired tissues in each group as previously reported.<sup>8</sup> Briefly, the biopsy samples (n = 6 knees derived from six rabbits respectively for each group) from repaired tissues were hydrated with circumfluent PBS at room temperature. The experiments were performed using the TriboIndenter system (Hysitron Inc., Eden Prairie, MN, USA) with a 100- $\mu$ m radius of a curvature cono-spherical diamond probe tip. Each indentation was force-controlled to a maximum indentation depth of 1000 nm. The samples were loaded for the first 10 seconds once the tips contacted the sample surface, held for 2 seconds at the maximum depth, and finally unloaded for 10 seconds.

### **1.13. Micro-CT Analysis of Subchondral Bone Reconstruction.**

At 3 and 6 months post-operation, rabbit femur end samples from each group (n = 12 knees at 3 months and n = 6 knees excepted for using to biomechanical assessment at 6 months) were subjected to micro-CT (GE, Boston, MA, USA) to evaluate subchondral bone reconstruction.<sup>9</sup> Samples were fixed for 24 h in 4% paraformaldehyde and placed in a sample holder for micro-CT scanning. A cylindrical region of interest 3 mm in diameter and 1.5 mm in thickness was selected to analyze the bone volume. The BMD and BV/TV were quantified.

### **1.14. Histomorphometry of Repaired Tissue.**

At 3 and 6 months post-operation, the rabbit knee samples (n = 12 knees at 3 months and n = 6 knees at 6 months, which had been examined by micro-CT) were decalcified in 10% (w/v) EDTA for 6 weeks at 37°C, embedded in paraffin, and cut into 7  $\mu$ m thick paraffin sections. The sections were stained with hematoxylin and eosin, Safranin-O/Fast Green, and Sirius red using a set of staining kits (all from Solarbio, Beijing, China) according to well-established standard protocols or according to the manufacturer's instructions.

For immunohistochemistry, the sections were treated with 0.25% pepsin (Abcam) at 37°C for 20

min for antigen retrieval. After washing with PBS, removing endogenous peroxidase with 3% hydrogen peroxide methanol solution and blocking nonspecific antigen with 10% goat serum, primary collagen II antibody (1:100, Cat# NBP2-33343; Novus) was applied overnight at 4°C. The next day, goat anti-mouse IgG (1:200; Cat# NB7539; Novus) was applied for 60 min. Subsequently, the nuclei were counterstained with hematoxylin. Photomicrographs were acquired using a Zeiss automatic digital scanning system (Carl Zeiss, Oberkochen, Germany).

To evaluate the progress of subchondral bone reconstruction and cartilage repair, sections from 12 knees at 3 months and 6 knees at 6 months per group (each sample represented three tissue sections) were blindly scored by three independent observers according to an established scoring system (Table S4 and S5).<sup>10</sup>

## 2. Supplemental Figure

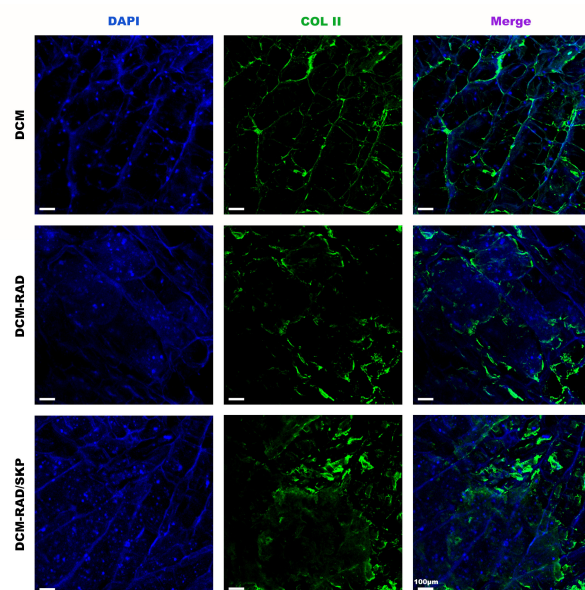


Figure S1. Representative anti-collagen type II immunofluorescence staining images of each group after 7 days *in vitro* mesenchymal stem cells (MSCs) recruitment.

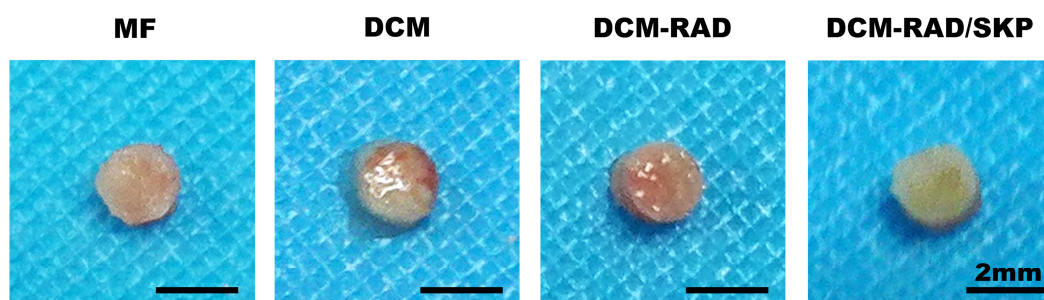


Figure S2. Representative macroscopic images of repaired tissue at 7 days after surgery.

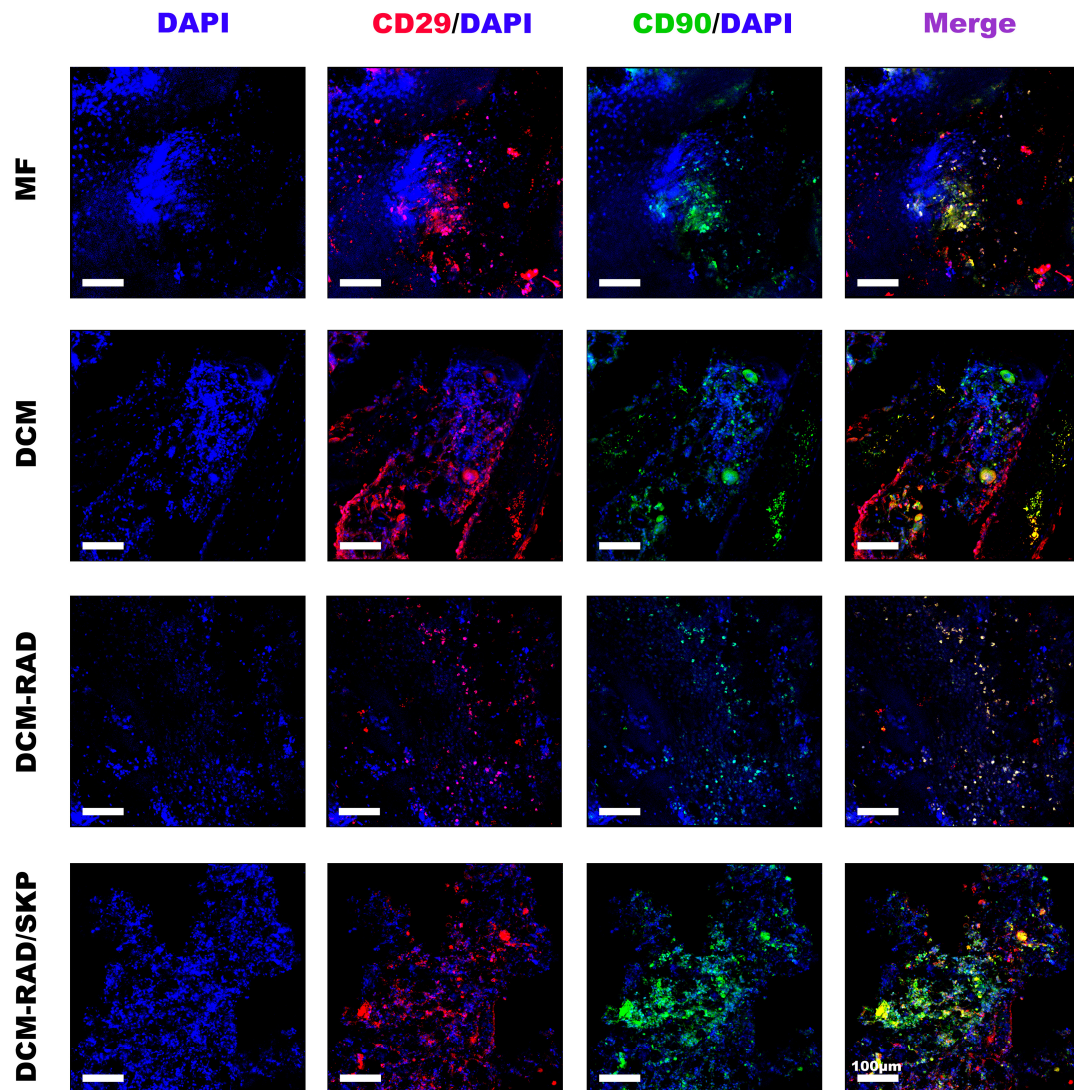


Figure S3. Representative maximum intensity projection confocal images of each group after 1 week *in vivo* implantation.

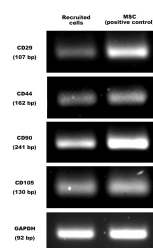


Figure S4. Semi-quantitative polymerase chain reaction (PCR) for mesenchymal stem cells (MSCs) marker CD29, CD44, CD90, and CD105 of recruited cell within each groups after 7 days *in vivo* implantation.



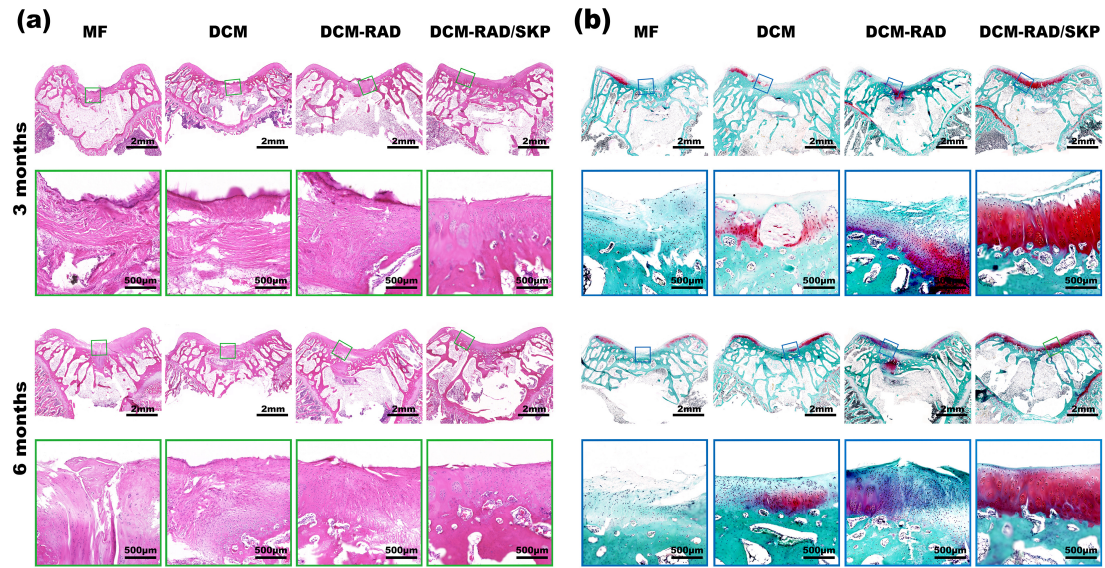


Figure S5. Histological evaluation of repaired tissue. (a) Representative hematoxylin and eosin staining of repaired knees at 3 and 6 months. (b) Representative Safranin-O/Fast Green staining of repaired knees at 3 and 6 months. Rectangles indicate the area shown on the lower panel images at higher magnification.

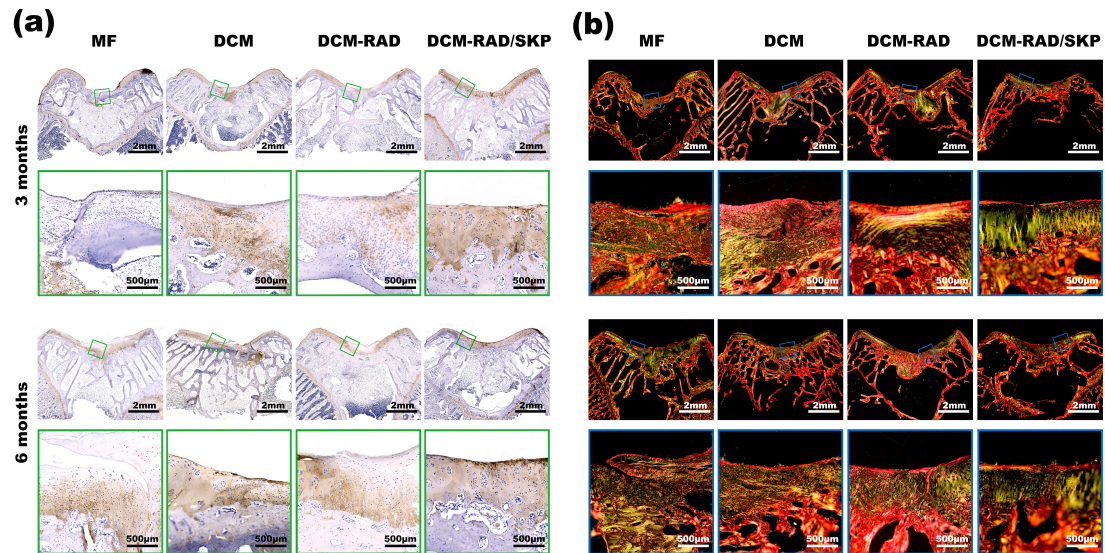


Figure S6. Cartilaginous matrix production, organization, and histological score. (a) Representative anti-collagen II immunohistochemical staining of repaired knees at 3 and 6 months. (b) Representative Sirius red staining of repaired knees at 3 and 6 months. Rectangles indicate the area shown on the lower panel images at higher magnification.

### 3. Supplemental Table

**Table S1.** Primers for semi-quantitative PCR analysis.

| Gene  | Forward primer (5'-3') | Reverse primer (5'-3') | Annealing temp (°C) | Product Size (bp) |
|-------|------------------------|------------------------|---------------------|-------------------|
| CD29  | CCCCATCGACCTCTACTACCT  | TCACCTCCTCATCTCATTCA   | 60                  | 107               |
| CD44  | AGGTTTGGTGGAAGACCTGG   | CTTCCTCCTCTGCCATGAGT   | 60                  | 162               |
| CD90  | ATTGCTTAGGGCTTATCCTTG  | CTTGCATCTGGGTCTTGAAG   | 60                  | 241               |
|       | TG                     | TG                     |                     |                   |
| CD105 | CAGCGTTGCGTCCTTCGTGG   | CGGGCTGCACCTGTTCTTC    | 60                  | 130               |
|       |                        | G                      |                     |                   |
| GAPDH | GAAGAAGGTGGTGAAGCAGG   | CACTGTTGAAGTCGCAGGA    | 60                  | 92                |
|       |                        | G                      |                     |                   |

Abbreviations: **CD**: Cluster of Differentiation; **GAPDH**: glyceraldehyde 3-phosphate dehydrogenase.

**Table S2.** Primers for RT-PCR analysis.

| Gene    | Forward primer (5'-3') | Reverse primer (5'-3') | Annealing temp (°C) |
|---------|------------------------|------------------------|---------------------|
| SOX9    | GCGGAGGAAGTCGGTGAAGAAT | AAGATGGCGTTGGGCGAGAT   | 57                  |
| COL10A1 | CCACCAGGACAAGCACTCAT   | CACTAACAAGAGGCATCCCG   | 57                  |
| COL2A1  | CACGCTCAAGTCCCTCAACA   | TCTATCCAGTAGTCACCGCTCT | 57                  |
| ACAN    | GGAGGAGCAGGAGTTTGTCAA  | TGTCCATCCGACCAGCGAAA   | 57                  |
| COL1A2  | GCCACCTGCCAGTCTTTACA   | CCATCATCACCATCTCTGCCT  | 57                  |
| GAPDH   | GAAGAAGGTGGTGAAGCAGG   | CACTGTTGAAGTCGCAGGAG   | 57                  |

Abbreviations: **SOX9**: transcription factor SOX9; **COL10A1**: collagen type X alpha 1; **COL2A1**: collagen type II alpha 1 **ACAN**: aggrecan; **COL1A2**: collagen type I alpha 2; **GAPDH**: glyceraldehyde 3-phosphate dehydrogenase.

**Table S3.** ICRS macroscopic morphology scoring system

| <b>Cartilage Repair Assessment ICRS</b>  | <b>Points</b> |
|--|---------------|
| Degree of defect repair  |               |
| In level with surrounding cartilage  | 4             |
| 75% repair of defect depth   | 3             |
| 50% repair of defect depth   | 2             |
| 25% repair of defect depth   | 1             |
| 0% repair of defect depth  | 0             |
| Integration to border zone   |               |
| Complete integration with surrounding cartilage  | 4             |
| Demarcating border < 1 mm  | 3             |
| Three-fourth of graft integrated, one-fourth with a notable border > 1 mm width            | 2             |
| Half of graft integrated with surrounding cartilage, and half with a notable border > 1 mm | 1             |
| Form no contact to one-fourth of graft integrated with surrounding cartilage               | 0             |
| Macroscopic appearance   |               |
| Intact smooth surface  | 4             |
| Fibrillated surface  | 3             |
| Small, scattered fissures, or cracks   | 2             |
| Several, small, or few but large fissures  | 1             |
| Total degeneration of grafted area   | 0             |
| Overall repair assessment  |               |
| Grade I: normal  | 12            |
| Grade II: nearly normal  | 11-8          |
| Grade III: abnormal  | 7-4           |
| Grade IV: severely abnormal  | 3-1           |

**Table S4.** Histological scoring system for evaluation of subchondral bone repair

| <b>Subchondral bone evaluation (within the bottom 1.5 mm of defect)</b> | <b>Points</b> |
|---|---------------|
| Percent filling with neo-formed tissue                                  |               |
| 100%  | 3             |
| > 50%   | 2             |
| < 50%   | 1             |
| 0%  | 0             |
| Subchondral bone morphology   |               |
| Normal, trabecular bone   | 4             |
| Trabecular bone, with some compact bone                                 | 3             |
| Compact bone  | 2             |
| Compact bone and fibrous tissue   | 1             |
| Only fibrous tissue or no tissue  | 0             |
| Extent of neo-tissue bonding with adjacent bone                         |               |
| Complete on both edges  | 3             |
| Complete on one edge  | 2             |
| Partial on both edges   | 1             |
| Without continuity on either edge                                       | 0             |

**Table S5.** Histological scoring system for evaluation of cartilage repair

| <b>Cartilage evaluation (within the upper 1 mm of defect)</b>              | <b>Points</b> |
|--|---------------|
| <b>Morphology of neo-formed surface tissue</b>                             |               |
| Exclusively articular cartilage  | 4             |
| Mainly hyaline cartilage   | 3             |
| Fibrocartilage (spherical morphology observed with $\geq 75\%$ of cells)   | 2             |
| Only fibrous tissue (spherical morphology observed with $< 75\%$ of cells) | 1             |
| No tissue  | 0             |
| <b>Thickness of neo-formed cartilage</b>                                   |               |
| Similar to the surrounding cartilage                                       | 3             |
| Greater than the surrounding cartilage                                     | 2             |
| Less than the surrounding cartilage  | 1             |
| No cartilage   | 0             |
| <b>Joint surface regularity</b>  |               |
| Smooth, intact surface   | 3             |
| Surface fissures ( $< 25\%$ neo-surface thickness)                         | 2             |
| Deep fissures ( $\geq 25\%$ neo-surface thickness)                         | 1             |
| Complete disruption of the neo-surface                                     | 0             |
| <b>Chondrocyte clustering</b>  |               |
| None at all  | 3             |
| $< 25\%$ chondrocytes  | 2             |
| 25-100% chondrocytes   | 1             |
| No chondrocytes present (no cartilage)                                     | 0             |
| <b>Chondrocyte and GAG content of neo-cartilage</b>                        |               |
| Normal cellularity with normal Safranin O staining                         | 3             |
| Normal cellularity with moderate Safranin O staining                       | 2             |
| Clearly less cells with poor Safranin O staining                           | 1             |
| Few cells with no or little Safranin O staining or no cartilage            | 0             |
| <b>Chondrocyte and GAG content of adjacent cartilage</b>                   |               |
| Normal cellularity with normal Safranin O staining                         | 3             |
| Normal cellularity with moderate Safranin O staining                       | 2             |
| Clearly less cells with poor Safranin O staining                           | 1             |
| Few cells with no or little Safranin O staining or no cartilage            | 0             |

#### 4. References

- (1) Liu, X.; Wang, X.; Wang, X.; Ren, H.; He, J.; Qiao, L.; Cui, F. Z. Functionalized self-assembling peptide nanofiber hydrogels mimic stem cell niche to control human adipose stem cell behavior in vitro. *Acta biomaterialia* **2013**, *9* (6), 6798-805, DOI: 10.1016/j.actbio.2013.01.027.
- (2) Yang, Q.; Peng, J.; Guo, Q.; Huang, J.; Zhang, L.; Yao, J.; Yang, F.; Wang, S.; Xu, W.; Wang, A.; Lu, S. A cartilage ECM-derived 3-D porous acellular matrix scaffold for in vivo cartilage tissue engineering with PKH26-labeled chondrogenic bone marrow-derived mesenchymal stem cells. *Biomaterials* **2008**, *29* (15), 2378-87, DOI: 10.1016/j.biomaterials.2008.01.037.
- (3) Kang, H.; Peng, J.; Lu, S.; Liu, S.; Zhang, L.; Huang, J.; Sui, X.; Zhao, B.; Wang, A.; Xu, W.; Luo, Z.; Guo, Q. In vivo cartilage repair using adipose-derived stem cell-loaded decellularized cartilage ECM scaffolds. *Journal of tissue engineering and regenerative medicine* **2014**, *8* (6), 442-53, DOI: 10.1002/term.1538.
- (4) Lu, J.; Sun, X.; Yin, H.; Shen, X.; Yang, S.; Wang, Y.; Jiang, W.; Sun, Y.; Zhao, L.; Sun, X. A neurotrophic peptide-functionalized self-assembling peptide nanofiber hydrogel enhances rat sciatic nerve regeneration. *Nano Research*, 1-15.
- (5) Mamisch, T. C.; Hughes, T.; Mosher, T. J.; Mueller, C.; Trattnig, S.; Boesch, C.; Welsch, G. H. T2 star relaxation times for assessment of articular cartilage at 3 T: a feasibility study. *Skeletal radiology* **2012**, *41* (3), 287-92, DOI: 10.1007/s00256-011-1171-x.
- (6) Huang, H.; Zhang, X.; Hu, X.; Shao, Z.; Zhu, J.; Dai, L.; Man, Z.; Yuan, L.; Chen, H.; Zhou, C.; Ao, Y. A functional biphasic biomaterial homing mesenchymal stem cells for in vivo cartilage regeneration. *Biomaterials* **2014**, *35* (36), 9608-19, DOI: 10.1016/j.biomaterials.2014.08.020.
- (7) Smith, G. D.; Taylor, J.; Almqvist, K. F.; Erggelet, C.; Knutsen, G.; Garcia Portabella, M.; Smith, T.; Richardson, J. B. Arthroscopic assessment of cartilage repair: a validation study of 2 scoring systems. *Arthroscopy : the journal of arthroscopic & related surgery : official publication of the Arthroscopy Association of North America and the International Arthroscopy Association* **2005**, *21* (12), 1462-7, DOI: 10.1016/j.arthro.2005.09.007.
- (8) Dai, L.; He, Z.; Zhang, X.; Hu, X.; Yuan, L.; Qiang, M.; Zhu, J.; Shao, Z.; Zhou, C.; Ao, Y. One-step repair for cartilage defects in a rabbit model: a technique combining the perforated decalcified cortical-cancellous bone matrix scaffold with microfracture. *The American journal of sports medicine* **2014**, *42* (3), 583-91, DOI: 10.1177/0363546513518415.
- (9) Yin, H.; Wang, Y.; Sun, Z.; Sun, X.; Xu, Y.; Li, P.; Meng, H.; Yu, X.; Xiao, B.; Fan, T.; Wang, Y.; Xu, W.; Wang, A.; Guo, Q.; Peng, J.; Lu, S. Induction of mesenchymal stem cell chondrogenic differentiation and functional cartilage microtissue formation for in vivo cartilage regeneration by cartilage extracellular matrix-derived particles. *Acta biomaterialia* **2016**, *33*, 96-109, DOI: 10.1016/j.actbio.2016.01.024.
- (10) Guo, X.; Park, H.; Young, S.; Kretlow, J. D.; van den Beucken, J. J.; Baggett, L. S.; Tabata, Y.; Kasper, F. K.; Mikos, A. G.; Jansen, J. A. Repair of osteochondral defects with biodegradable hydrogel composites encapsulating marrow mesenchymal stem cells in a rabbit model. *Acta biomaterialia* **2010**, *6* (1), 39-47, DOI: 10.1016/j.actbio.2009.07.041.